Chemistry & Biology, Vol. 12, 89–97, January, 2005, ©2005 Elsevier Ltd All rights reserved. DOI 10.1016/j.chembiol.2004.11.007

Enhanced Ligand Affinity for Receptors in which Components of the Binding Site Are Independently Mobile

Clare R. Trevitt,[1] C. Jeremy Craven,[1] Lilia Milanesi,[1,2] Karl Syson,[1] Maija-Liisa Mattinen,[1,3] Julie Perkins,[2] Arto Annila,[4] Christopher A. Hunter,[2] and Jonathan P. Waltho[1,*]

[1]Krebs Institute for Biomolecular Research
Department of Molecular Biology and Biotechnology
University of Sheffield
Sheffield S10 2TN
United Kingdom

[2]Krebs Institute for Biomolecular Research
Department of Chemistry
University of Sheffield
Sheffield S3 7HF
United Kingdom

[3]VTT Biotechnology
Espoo FIN-02044
Finland

[4]Institute of Biotechnology
Department of Physical Sciences
University of Helsinki
Helsinki FIN-00014
Finland

Summary

Using calmodulin antagonism as a model, it is demonstrated that, under circumstances in which binding sites are motionally independent, it is possible to create bifunctional ligands that bind with significant affinity enhancement over their monofunctional counterparts. Suitable head groups were identified by using a semiquantitative screen of monofunctional tryptophan analogs. Two bifunctional ligands, which contained two copies of the highest-affinity head group tethered by rigid linkers, were synthesized. The bifunctional ligands bound to calmodulin with a stoichiometry of 1:1 and with an affinity enhancement over their monofunctional counterparts; the latter bound with a stoichiometry of 2:1 ligand:protein. A lower limit to the effective concentrations of the domains of calmodulin relative to each other (0.2–2 mM) was determined. A comparable effective concentration was achieved for bifunctional ligands based on higher-affinity naphthalene sulphonamide derivatives.

Introduction

A successful strategy to design ligands to biological macromolecules, which have both high affinity and high specificity, is to link together two lower-affinity ligands [1, 2]. Such an affinity enhancement, however, is by no means assured [3, 4]. It depends on (1) how much the binding conformation of the macromolecule is perturbed away from the optimum given the restraints imposed by accommodating the linked compound, (2) how large an entropic loss in the target molecule is required by the binding, and (3) how much flexibility the linked compound is required to lose in the linker upon binding. All of these components combine to determine the effective concentration for the second interaction. The magnitude of this effective concentration, C_{eff}, is reflected in any enhanced affinity of the bifunctional ligand over the corresponding monofunctional ligands and is given by:

$$C_{eff} = \frac{K_d^A K_d^B}{K_{AB}} \quad (1)$$

where A and B represent two moieties of a bifunctional ligand, AB, for which the dissociation constants as monofunctional ligands (K_d^A and K_d^B) are known. To achieve simultaneous binding of, for example, two domains to one ligand, the value of C_{eff} needs to be larger than the dissociation constant of the weaker binding monofunctional moiety. In this scenario, C_{eff} is also the concentration at which the formation of linear polymers of receptors linked by bifunctional ligands begins to compete effectively with 1:1 binding. Thus, if the value of C_{eff} can be determined (or at least a lower limit of its value), this provides a quantitative measure of the minimum affinity that must be achieved by the component moieties of a bifunctional ligand, if binding in a bifunctional mode is to provide an improvement in affinity. As an example, for a protein that binds to a monofunctional ligand with a dissociation constant of 1 μM, a C_{eff} value greater than 1 μM will ensure that the simultaneous participation of both domains in a complex with the target is the preferred state (Equation 2).

$$\text{Enhancement of bifunctional binding} = \frac{K_d^A}{K_d^{AB}} = \frac{C_{eff}}{K_d^A} \quad (2)$$

To date, applications of linked bifunctional ligands for biological macromolecular receptors have focused on macromolecules containing adjacent ligand binding sites that are in a fixed positional relationship to one another. Reported examples of linked ligands include a wide variety of multisubstrate analogs, including bisubstrate analog inhibitors for a range of enzymes. For example, the design of linked ligands was developed empirically based on models of transition state complexes involving two substrates and has led to affinity enhancements of 2–5 orders of magnitude [5–10]. Multisubstrate ligands also largely involve rigid linkers, including examples that have been either designed [11] or selected by combinatorial methods [12] to be closely complementary to protein sites that, again, have fixed positional relationships. An alternative strategy, developed for a homo-multimeric protein with binding sites in fixed positional relationships [13], utilizes highly flexible linkers between two ligand moieties. The linkers do not become immobilized upon binding, but determine, according to their length, the effective concentration of the two head groups.

The use of bifunctional ligands for multidomain proteins that have ligand binding sites that are not fixed in position relative to each other, though, has been largely

*Correspondence: j.waltho@shef.ac.uk

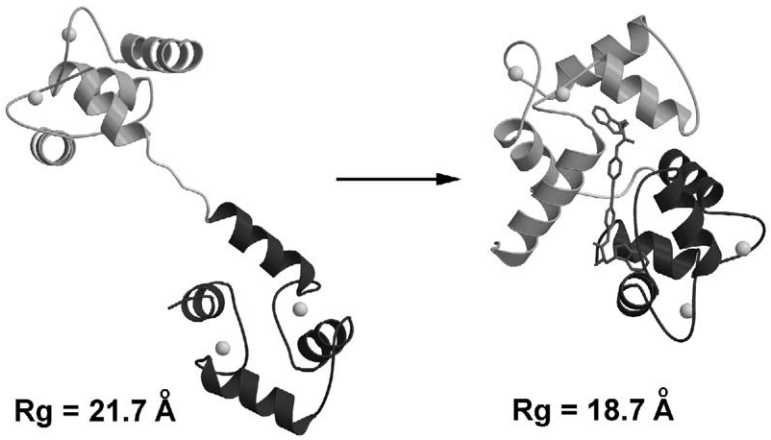

Figure 1. A Schematic Representation of the Closure of CaM in Response to a Bifunctional Ligand

Calcium-loaded CaM (left) displays motional independence of the two domains, each of which has a hydrophobic pocket capable of binding a tryptophan moiety. In order to accommodate the bifunctional ligands consisting of two linked tryptophan head groups (right), CaM is required to form a closed conformation. The models are based on the pdb entries 3cln (left) and 1cll (right), with the bifunctional ligand inserted with MACROMODEL [49]. The picture was generated with MOLSCRIPT [50] and Raster3D [51]. Below each model is the radius of gyration for the state determined from small-angle X-ray scattering distribution functions (see Figure 5) recorded on both 0.5 mM CaM and a 0.5 mM 1:1 complex between CaM and ligand BT1 (see Figure 2B).

overlooked [14]. However, a corollary of the successful use of flexible ligands for rigid binding sites [13] is that it should be achievable to attain increased binding affinity to proteins with motionally independent binding sites by using ligands connected by fixed linkers, if a sufficiently high effective concentration can be attained. Although effective concentrations as high as 10–100 M have been reported for complexes between bidentate ligands and nonprotein receptors in which the binding site orientations are fixed, these values are greatly reduced for the equivalent compounds in complexes in which the binding sites have relative motion [15]. In addition, the reported effective concentrations attained between linked ligands and proteins rarely approach the values attained for nonprotein receptors, even when the binding sites have relatively fixed orientations and positions [1]. Therefore, if bifunctional ligands with enhanced affinity are to be developed for binding sites that are not in fixed relative positions, it is important to establish a strategy by which the effective concentration of a second interaction can be readily measured in order to ascertain whether linked ligands are likely to be an improvement over their monofunctional counterparts.

Here, we show how a limit on C_{eff} can be readily established for a protein, in which the ligand binding sites are motionally independent, by using small, rigid, linked ligands. We illustrate the strategy by using the ubiquitous calcium signal transducer calmodulin (CaM) as a representative example (Figure 1). CaM is comprised of two highly homologous domains, each of which contains a hydrophobic surface, exposed upon binding of calcium ions [16–18], and binds to a variety of hydrophobic, small-molecule antagonists [19, 20]. The binding of numerous such monofunctional ligands has been characterized both thermodynamically and structurally [21–25]. Motional independence between the two domains when CaM is unliganded has been clearly demonstrated [26–28], and the protein is known to use both domains in the binding of recognition sequences of target proteins in a closed conformation [29–31], implying that a high value of C_{eff} can be achieved despite the relative motion of the unliganded form. However, the value of C_{eff} has not been established for the peptide (or antagonist) complexes of CaM, and the attainment of an equivalently high effective concentration with small, linked ligands is not guaranteed for the reasons outlined above. In terms of ligand design, the structural similarity of the two antagonist binding sites in CaM allowed us, in this case, to utilize symmetric bifunctional ligands, and the established ability of CaM to accommodate target peptides of different lengths [30] enabled us to synthesize a limited number of bifunctional ligands with predominantly rigid linkers of different lengths between the two recognition moieties. In general, though, the strategy can be equally applied to asymmetric ligands and a far wider series of linkers that are synthesized either individually or combinatorially and selected on the basis of affinity for the target protein.

Results

In order to establish a value for C_{eff} with bifunctional ligands, the dissociation constants of the monofunctional components from which the bifunctional ligand is constructed need only to exceed C_{eff}. In other words, in the scenario in which C_{eff} is high (e.g., in the millimolar range), and therefore in which the use of bifunctional ligands could be highly advantageous, the affinity for the target of the monofunctional components used to measure C_{eff} can be relatively low, i.e., the ligands that are linked can be relatively poor models of the optimum binding moiety or head group.

Peptide-Mimic Ligands

In the case of CaM, the first generation of bifunctional ligand that was investigated was based simply on the amino acid tryptophan, which is a component of many natural CaM target peptides, but only part of the moiety that contacts the hydrophobic surface on each of the CaM domains. Tryptophan is a convenient choice from a chemical perspective in that it possesses spectroscopic properties that are not present in CaM and it has the potential for simple functional group modifications through which to attach a linker. Tryptophan also broadly

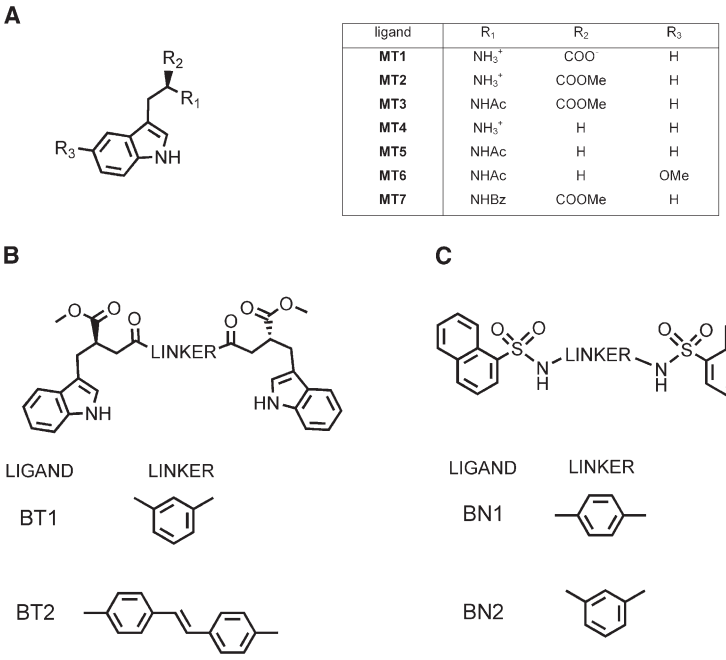

Figure 2. The Structures of the Ligands

(A) Monofunctional tryptophan (R_2 = COOR) and tryptamine (R_2 = H) ligands.

(B) The peptide-mimic bifunctional ligands, comprising two linked MT2 moieties.

(C) The second-generation bifunctional ligands, based on naphthalene sulphonamide head groups.

conforms to the CaM antagonist paradigm [19], which constitutes a hydrophobic, aromatic head with a basic tail. For CaM, the number of compounds synthesized could be limited owing to the wealth of structural information already available, and, therefore, the measurement of C_{eff} is simplified experimentally by removing the need to make many compounds and separate them according to their affinity. The three-dimensional structures of CaM-target peptide complexes show that tryptophan side chains bind within a well-defined pocket in the hydrophobic surface of each CaM domain; the two pockets are separated by more than 20 Å. Thus, it was likely that bifunctional ligands based on two tryptophan moieties should be accommodated by CaM without the introduction of substantial strain into the protein.

Using 1D ^{1}H NMR and ligand fluorescence, an initial semiquantitative screen of a family of homologous, monofunctional, tryptophan-based ligands, MT1–MT6 (Figure 2A), was carried out to select which variant of the tryptophan moiety was the most suitable head group for the construction of bifunctional ligands (Figure 2B). The most reliable estimate of the relative binding affinities of the ligands was obtained by using pulsed gradient spin echo (PGSE) NMR experiments [32]. These were performed on samples with ligand:protein concentration ratios of 2:1, and the spectra were edited according to the translational diffusion properties of the protein. The resulting resonances reflect the population of ligand that is not bound to the protein. In Figure 3A, three examples of such diffusion-edited spectra are shown, in comparison with the spectra of the free ligands. The chemical shift changes that occurred upon addition of protein to ligand solutions were in the NMR fast-exchange regime. Resonances from both CaM domains were affected simultaneously by ligand binding and followed identical binding isotherms, indicating similar binding affinities for the two domains, as observed previously for a range of monofunctional ligands [23]. In Figure 3B, the amplitudes of the chemical shift changes observed upon binding for representative nuclei in both the protein and the ligand are summarized. These data illustrate the general trend that larger changes in chemical shift are associated with higher-affinity binding, as determined by the PGSE data. For ligands MT1 and MT6, the very small perturbation of chemical shifts and the high residual signal intensity in diffusion-edited spectra indicates the absence of significant interaction with CaM at millimolar concentrations. For MT2–MT5, all probes indicate significant interaction with CaM, with MT2 and MT3 showing the strongest effects. The MT2/MT3-type head group was therefore selected for the synthesis of bifunctional ligands.

Based on the structures of CaM in complex with peptide models of protein targets [29–31], the approximate lengths of linkers that would accommodate the domain separation of a closed form of CaM were estimated (Figure 1). Two bifunctional ligands (Figure 2B) were synthesized, each containing two identical tryptophan head groups tethered by predominantly rigid linker groups. A quantitative analysis of the binding affinity was initially carried out by using NMR for the ligands BT1, MT2, MT3, and MT7, the last being a "mono + linker" ligand designed to probe the effects attributable solely to the linker group (Figure 2). Again, the binding of all ligands to CaM was in the NMR fast-exchange regime. Examples of changes in chemical shift as the ligand:CaM ratio is increased are shown for a mono- and a bifunctional ligand in Figure 4A, and the derived dissociation constants and stoichiometries for each are summarized in Table 1.

Importantly, ligand BT1 has a 1:1 stoichiometry with CaM, compared to the 2:1 stoichiometry of the monofunctional ligands, including MT7. For BT1, protein chemical shift changes were complete by 1.0 ligand

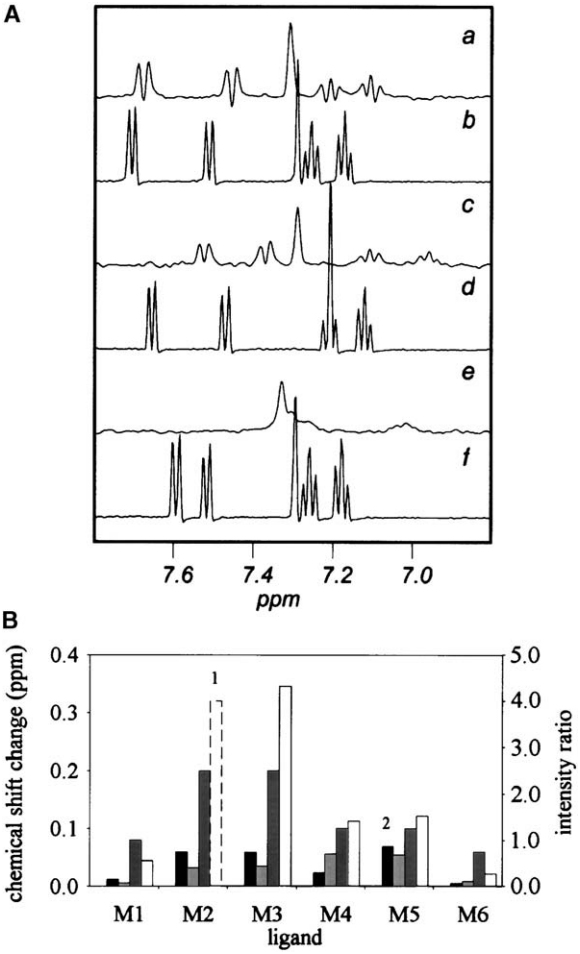

Figure 3. NMR Screen of Ligand Binding

(A) Aromatic region of diffusion-edited ^{1}H NMR spectra for 1 mM CaM samples containing two ligand equivalents (a, c, e), in comparison with free ligand spectra (b, d, f) for ligands (a and b) MT1, (c and d) MT4, and (e and f) MT2. Free ligand spectra were acquired by using 5 mM samples in D_2O (MT1, MT2) or 20% d_3-MeOH (MT4).

(B) Summary of NMR probes indicative of interaction between CaM and ligands MT1–MT6. For each measurement, larger bars indicate higher-affinity binding. Protein chemical shifts (black bars) and ligand indole NH chemical shifts (light-gray bars) were measured from initial-final chemical shifts in the titration of five aliquots of 0.5 equivalents of ligand into 1 mM CaM. Diffusion-edited spectra were derived from experiments acquired at 0% and 100% (50W) gradient strength. The intensity of the diffusion-edited spectrum is given relative to the intensity of the PGSE spectrum with 0% gradient power (dark-gray bars, right vertical scale). The average chemical shift changes for aromatic ligand resonances (white bars) were measured from the difference between the diffusion-edited spectrum and the free ligand spectrum for identifiable signals. [1]Average ligand chemical shifts are the lower limits for MT2, due to very low-intensity signals. [2]For MT5, the protein chemical shift change is an estimated maximum value, since protein I27 NH and ligand indole NH resonances converge upon increasing ligand:CaM ratios.

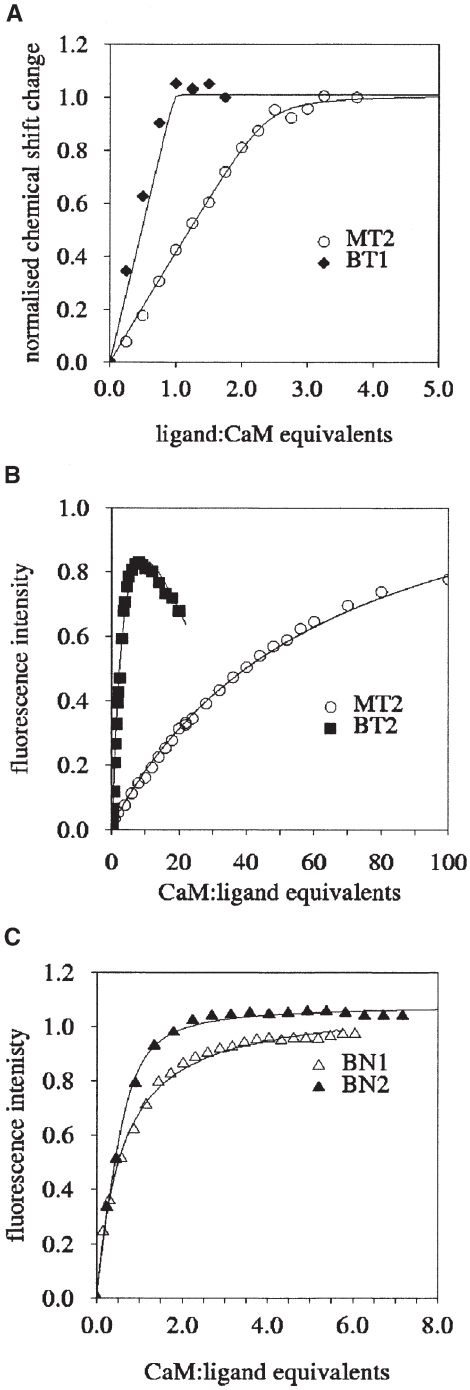

Figure 4. Plots Showing the Change in Observed Signal for Representative Titrations, Together with the Lines of Best Fit Obtained by Least-Squares Fitting of the Data

(A) Normalized NMR chemical shift changes for CaM I27 amide resonance upon addition of ligands MT2 (open circles) or BT1 (filled diamonds).

(B) Normalized fluorescence changes observed upon addition of CaM to peptide-mimic ligands MT2 (open circles) or BT2 (filled squares), monitored at 350 nm and 460 nm, respectively. For consistency in reported fluorescence changes, the observed values for the BT2 experiment (decreasing fluorescence) are inverted relative to those for MT2 (increasing fluorescence).

(C) Normalized fluorescence changes observed upon addition of CaM to ligands BN1 (open triangles) and BN2 (filled triangles) monitored at 550 nm.

equivalent, indicating that the dissociation constant is at least two orders of magnitude less than the protein concentration (i.e., the strong binding limit). None of the monofunctional ligands were at this limit. Although an accurate dissociation constant for BT1 cannot there-

Table 1. Dissociation Constants and Stoichiometries for Interactions between CaM and Representative Monofunctional and Bifunctional Ligands

Ligand	K_d (μM)	Stoichiometry (Ligand:CaM)	Method of K_d Determination
MT2	400 ± 100	2	NMR, fluorescence, ITC
MT3	150 ± 60	2	NMR
MT7	60 ± 25	2	NMR
BT1	~10	1	NMR, ITC
BT2	9 ± 6	1	Fluorescence
BN1	0.07 ± 0.05	1	Fluorescence
BN2	0.01 ± 0.008	1	Fluorescence

fore be determined directly from this titration, the weakest affinity possible corresponds to a dissociation constant of ~10 μM, whereas the fast exchange of NMR resonances from the free and bound species indicates that the strongest affinity possible is no greater than 1 μM. NMR-monitored titrations at CaM concentrations below the strong binding limit were supportive of a dissociation constant in the range of 1–10 μM, but a more precise value could not be obtained owing to limitations in sensitivity. Stoichiometric addition of bifunctional ligands to CaM induces its transformation to a closed form (Figure 1), as determined by small-angle X-ray scattering. For example, the radius of gyration of CaM falls from 21.7 to 18.7 Å upon binding of BT1 (Figure 5). This change compares closely with the fall in the radius of gyration when comparing previously reported values for unliganded CaM and for 1:1 MLCK-I + CaM [33, 34].

Although the incorporation of tryptophan moieties was intended to allow the use of ligand fluorescence for the determination of higher-affinity dissociation constants, the indole fluorescence is completely quenched by the linker group in BT1 and is largely quenched in BT2. Only a low-intensity fluorescence signal with maxima at 380 and 460 nm could be observed for the latter. From a titration of CaM into BT2 monitored by fluorescence (Figure 4B), the measured dissociation constant for the 1:1 interaction is approximately 9 μM (Table 1).

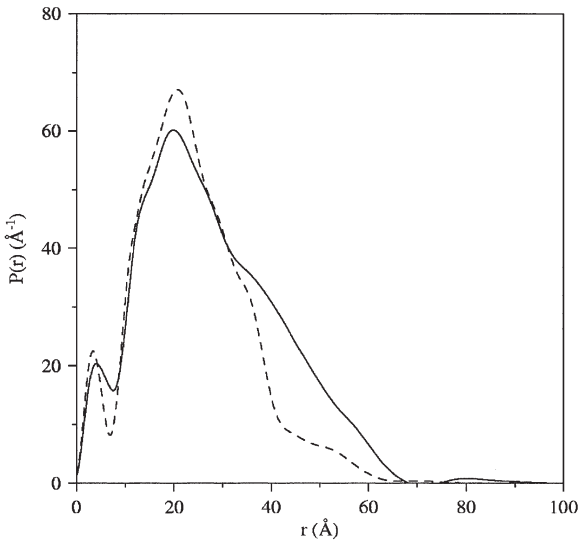

Figure 5. SAXS Measurements of Unliganded and Bifunctional Ligand Bound CaM

A comparison of the distance distribution P(r) functions for calcium-loaded CaM (solid line) and a 1:1 complex of BT1 and calcium-loaded CaM (broken line), illustrating the compaction that occurs upon binding of the bifunctional ligands. The radius of gyration falls from 21.7 Å to 18.7 Å upon formation of a 1:1 complex.

For the bifunctional ligand BT1, ligands MT3 and MT7 can be used to represent its two component moieties in the determination of C_{eff}. BT1 binds with an affinity enhancement of between 1 and 2 orders of magnitude over MT3, and a factor of 5 over MT7 (Table 1). Importantly, the stoichiometry difference between the bifunctional and the mono + linker ligand, MT7, indicates that it is the second head group moiety, rather than the presence of the linker group, that causes the bifunctional binding. Using the derived dissociation constants (Table 1), C_{eff} for the domains of CaM for BT1 is in the range of ~0.2–2 mM. The length of the linker groups in BT1 and BT2 was found to make little difference to the binding affinity, as predicted from the ability of CaM to accommodate peptides with different relative positions of the side chains that bind to its hydrophobic surfaces.

In principle, the major contribution of C_{eff} to the binding affinity is usually ascribed to an entropy term that favors binding for bifunctional ligand-CaM complexes. To test whether the increase in binding affinity for the bifunctional ligands is largely the result of such an entropy term, isothermal titration calorimetry (ITC) was used to measure the changes in enthalpy (ΔH), and hence entropy (ΔS), upon binding for ligands MT2 and BT1. The dissociation constants measured by ITC (Table 2) match within error those measured by other methods (Table 1). Over the temperature range of 8°C–37°C, ΔH and ΔS were negative for binding of both ligands, and the negative values of ΔC_p imply a significant hydrophobic contribution to the binding free energy. The value of ΔH for the bifunctional ligand is twice that for the monofunctional ligand (within error), which suggests that there is no substantial change in the individual binding interactions at the two sites. However, ΔS for binding the bifunctional ligand is also twice (within error) that for the monofunctional ligand; thus, it is not possible to identify an unambiguous entropic contribution to C_{eff}.

Dissecting these factors is a major challenge, so it is impossible to reliably assign the cooperativity to an entropy or enthalpy effect in this system.

The problem is that there are several different factors

Table 2. Thermodynamic Parameters for Monofunctional and Bifunctional Ligand Binding to CaM Measured by ITC at 25°C

	MT2 1:1 Monofunctional Complex	BT1 1:1 Bifunctional Complex
K_d (μM)	600 ± 100	8 ± 1
ΔG (kJ mol^{-1})	−18.3 ± 0.5	−28.6 ± 0.5
ΔH (kJ mol^{-1})	−35 ± 3	−64 ± 1
TΔS (kJ mol^{-1} K^{-1})	−16 ± 3	−36 ± 1
ΔC_p (J mol^{-1} K^{-1})	−1700 ± 900	−2600 ± 700

that can contribute to the observed enthalpy and entropy changes. For the monofunctional ligand these are:

1. Binding interactions. These could make a favorable contribution to ΔH.
2. Hydrophobic effects. These could make a favorable contribution to ΔS and an unfavorable contribution associated with the desolvation of polar groups.
3. Restricting intermolecular motion. This will make an unfavorable contribution to ΔS [35].
4. Conformational changes in the protein and/or the ligand. These can make favorable or unfavorable contributions to ΔH and ΔS. Structural tightening could make ΔH and ΔS more negative, or structural loosening would make ΔH and ΔS more positive. These compensatory changes in ΔH and ΔS are often very large relative to the size of the effect discussed here [36].

For the bifunctional ligand, the magnitude of these effects will differ from the monofunctional system. The contributions from (1) and (2) should be approximately double those for the monofunctional ligand, and the contribution from (3) should be similar. However, in the bifunctional case, there is additional restriction of the conformations of the linkers between the two protein domains and the tryptophan moieties that will compensate the entropic advantage of the bifunctional ligand to some extent.

Naphthalene Ligands

Despite the relatively low affinity of tryptophan-based monofunctional ligands, the range measured for C_{eff} is sufficient to lead to a modest affinity enhancement for the equivalent bifunctional ligands. However, if this range of C_{eff} can be maintained, it follows from Equation 1 that a larger enhancement of affinity should be achievable for bifunctional ligands starting from monofunctional moieties with higher affinities than MT1–MT7. To demonstrate this, a second generation of bifunctional ligands, BN1 and BN2 (Figure 2C), was synthesized. In this generation of ligands, the linkers were based on the peptide-mimic bifunctional ligands, but two naphthalene sulphonamide head groups were used in place of the tryptophan moieties. Naphthalene sulphonamides bind to the same sites of CaM as tryptophan derivatives, as indicated by the distribution of chemical shift changes in the protein upon addition of ligand [23, 24], and are a feature of numerous monofunctional CaM antagonists that bind with dissociation constants in the range of 1–10 μM [19, 23, 24], i.e., 1–2 orders of magnitude more strongly than the monofunctional tryptophan derivatives. The linker groups were chosen to give overall ligand lengths comparable to the tryptophan-based bifunctional ligands. The dissociation constants for BN1 and BN2 were determined to be 70 nM and 10 nM, respectively (Table 1), by using changes in intrinsic fluorescence of the ligand at 550 nm upon titration of CaM into a solution of the ligand. The stoichiometry for each binding event was confirmed as 1:1 by using a titration of ligand to CaM at concentrations of ten times the determined dissociation constants.

Thus, the simple bifunctional derivative BN2 binds to CaM with a 1:1 stoichiometry and an affinity approaching that of peptides corresponding to the natural recognition target of CaM. This affinity is some 2–3 orders of magnitude stronger than that of any monofunctional ligand equivalent and indicates that this second generation of ligand was no more limited in C_{eff} by the linker design than the tryptophan-based bifunctional ligands. In other words, on the basis of the range determined for C_{eff} by using the tryptophan-based bifunctional ligands, it was straightforward to design a bifunctional ligand that greatly exceeded its monofunctional counterparts in affinity and that binds CaM in competition with its physiological partners.

Discussion

From the example of ligand binding to CaM, it is clear that ligands that are bound to biological macromolecules with enhanced affinity can be derived by the linking together of two lower-affinity ligands even when the binding sites are mobile relative to each other. The degree of affinity enhancement is related to the effective concentration, C_{eff}, of the second binding event, a quantity that can be readily determined by using simple, low-affinity head groups connected by relatively rigid linkers. The monofunctional tryptophan-based ligands that were linked in the present study and that were sufficient to determine the value of C_{eff} for CaM have a low affinity for CaM (Table 1), and this affinity is considerably lower than traditional monofunctional CaM antagonists, such as J-8 and trifluoperazine. Relative to the latter, binding is likely to be disfavored by the indole NH group of the tryptophan moiety that constitutes a hydrogen bonding potential that is not present in the other ligands, and that is not satisfied by the ligand binding site. The absence of a significant change in the chemical shift of the indole NH resonance upon binding (see Figure 3B) supports this, indicating that its solvation state is retained in the complex.

Paradoxically, ligand MT6 is melatonin, a neurotransmitter reported to inhibit CaM-dependent activation of some enzymes [37] and to have a picomolar dissociation constant for CaM [38], i.e., even stronger binding than the nano-molar affinities of target enzymes for CaM [39]. However, in agreement with data from a previous study [40], the results obtained here reveal a dissociation constant weaker than 1 mM for melatonin and indicate that substitution of the indole ring further disfavors binding to CaM. Furthermore, the weak interaction of ligand MT1 with CaM compared to the stronger binding of ligands MT2 and MT3 suggests that it is not the presence of a positive charge that favors

CaM binding, as proposed in the paradigm molecule [19], but that a negative charge is detrimental to binding.

The range of C_{eff} values determined here (0.2–2 mM) represent a lower limit for that achievable for the domains of CaM. Despite each linker in the bifunctional ligands being predominantly rigid, six rotatable bonds separate the two indole moieties in the tryptophan-derived bifunctional ligands, and four rotatable bonds separare the moieties in the naphthalene sulphonamide bifunctional ligands. Although this flexibility may help alleviate constraints imposed by suboptimal orientation and separation of the head groups, any restriction of rotors would ameliorate the benefits, leading to a compromise in affinity enhancement and a corresponding lowering of C_{eff}. Naturally, ligands requiring the restriction of too many rotors or with inappropriately oriented or separated head groups will have effective concentrations below the dissociation constant of the corresponding monofunctional ligands; thus, 2:1 stoichiometry binding will dominate the equilibrium, and any affinity enhancement is lost. Conversely, more rigid ligands with appropriate head group orientation and separation have the potential for considerably enhanced affinity over that reported here.

As would be expected for many multidomain proteins, a relatively high effective concentration of the two domains of CaM is reflected in its mode of action. The coupling of the two domains by the tether limits the free energy loss resulting from the conformational selection required to bring the two domains together upon formation of complexes with the target proteins. The cooperative behavior of the two domains at cellular calcium levels is also further moderated by the differences in their calcium affinities [41]. Moreover, CaM accommodates multiple target proteins that present a variety of binding regions. Interdomain flexibility is a convenient means of relaxing the constraints on substrate specificity, while tethering maintains a large enough effective concentration to illicit cooperative binding. The CaM system also restricts its free energy loss upon cooperative binding of the two domains by the behavior of the tether in the CaM-peptide complexes. Upon binding peptides, not all of the region between the two domains is conformationally frozen, evidenced by the absence of electron density in this region in the crystal structure of the CaM-CaMKII peptide complex [30]. Overrestriction of the tether would diminish the affinity of the two-domain complex in an analogous manner to the overrestriction of rotamers in the bifunctional ligands described above.

Significance

The results presented here for CaM clearly illustrate the value in utilizing linked ligands for enhancing the binding affinity of ligands to proteins with motionally independent binding sites, and the value of quantifying a lower limit on the achievable effective concentration for multidentate interactions by using simple head groups with, in this case, millimolar dissociation constants. While the mechanism of action of CaM strongly hints at the potential advantage of using bifunctional ligands, which turned out to be highly successful, many systems for which an equivalent strategy could be equally successful will not be so well defined in terms of structure and affinity measurements. Nevertheless, knowledge about any independent ligand binding properties, regardless of any apparent relative motion of the parts of the protein involved in that binding, should be sufficient to design simple, linked ligands with which to test the achievable values of C_{eff} in an analogous manner to that described above for CaM. In other words, the observation of relative motion between potential ligand binding sites should not deter the investigation of linked ligands as high-affinity derivatives. The nature of the tether between the ligand binding sites can maintain considerable relative proximity.

Experimental Procedures

Materials

All ligands (Figure 2) are named with a prefix "XY," according to their class, where X = M or B depending on whether the ligand is monofunctional or bifunctional, respectively, and Y = T or N depending on whether the head group is based on tryptophan or naphthalene, respectively. Ligands MT1 (L-tryptophan), MT2 (L-tryptophan methyl-ester, hydrochloride salt), MT4 (tryptamine), and MT6 (5-methoxy-*N*-acetyl tryptamine) were obtained commercially and were used without further purification.

Ligand Synthesis

Modifications to ligands MT2 and MT4 were performed by using the following protocol, where the term "acid chloride" refers to the acetyl chloride for acetylation (MT2 → MT3, MT4 → MT5) or the benzoyl chloride for benzoylation (MT2 → MT7) reactions. A total of 1 mmol of the free amine (MT2 or MT4) was dissolved in dry dichloromethane (DCM) with two equivalents of triethylamine (Et_3N); one equivalent of the acid chloride was then added dropwise at 0°C. The reaction mixture was stirred at room temperature for 1 hr. The organic phase was washed in 1 M HCl, washed to neutral with H_2O, and dried over anhydrous sodium sulfate (Na_2SO_4). Where necessary, further purification was achieved by silica gel chromatography in 9:1 ethyl-acetate:petroleum-ether solution. The products were recrystallized by slow diffusion of petroleum ether into DCM.

The synthesis for bifunctional ligands BT1 and BT2 involved the coupling of two MT2 moieties by a di-acid chloride linker molecule using a method analogous to the *N* modifications described above. The acid chlorides corresponding to the di-acid linkers (Figure 2B) were formed by activation of the di-acid with oxalyl chloride, by using DCM as solvent and dimethylformamide (DMF) as a catalyst. A total of 2 mmol MT2 was dissolved in dry DCM with two equivalents of Et_3N. 0.5 equivalents of the acid chloride was added stepwise at 0°C. The reaction was left stirring at room temperature for 12 hr, and the products were isolated as described above.

The method used for the synthesis of the bifunctional naphthalene sulphonamide ligands is a modification of a previously published protocol [42]. Ligands BN1 and BN2 (Figure 2C) were synthesized by linking two 1-naphthalene sulphonylchloride moieties with p-xylylenediamine or m-xylylenediamine, respectively. A total of 1 mmol xylylenediamine was dissolved in 7.5 ml dry DCM, and three equivalents of Et_3N were added under nitrogen (N_2). A total of 2 mmol 1-naphthalene sulphonylchloride was dissolved in an equivalent volume of dry DCM and added dropwise to the xylylenediamine/Et_3N mixture at room temperature under N_2. The reaction was left stirring at room temperature overnight under N_2. The reaction mixture was then washed in 1 M sodium hydroxide (aqueous), and the organic layer was removed. The aqueous layer was further washed twice with dry DCM. All organic washes were pooled and dried over anhydrous Na_2SO_4. The products were recrystallized by slow diffusion of hexane into DCM.

The characterization of each new compound by NMR and ele-

mental analysis is provided in the Supplemental Data (available with this article online). Stock solutions of the ligand samples were prepared by dissolution of recrystallized material in water, MeOH, or DMSO as appropriate.

CaM Preparation

Protein samples were prepared from lyophilized recombinant mammalian CaM [43–45] by dissolution in 50 mM KCl, 10 mM $CaCl_2$, 0.5 mM NaN_3 (pH 6.0). Protein concentrations were quantified by titration with Ca^{2+} monitored by ^1H NMR. All experiments were carried out at 298K.

NMR Spectroscopy

Spectra were acquired with Bruker AMX-500 or DRX-500 spectrometers. Spectral widths were 12,500 Hz, and relaxation delays were typically 0.7 s for protein spectra and 3 s for ligand spectra. Solvent suppression was achieved by using presaturation. PGSE experiments [32] included a composite 180° pulse to refocus the magnetization in the center of a delay between two identical gradients. Sine-shaped gradient pulses of 8 ms duration were used, with a center-to-center separation of 10.7 ms. Experiments were acquired at 0% and 100% gradient strength in order to obtain diffusion-edited spectra [46]. All experiments were acquired with a 2.5 ms preacquisition Hahn echo [47], and the water resonance was removed with a convolution difference filter by using FELIX (Accelrys, San Diego).

Fluorescence Spectroscopy

Experiments were performed with HITACHI-4500 and Shimadzu RF-5301 fluorescence spectrophotometers. For the peptide mimic ligands MT2 and BT2, fluorescence emissions between 300 and 400 nm upon excitation at 295 nm (MT2) or between 335 and 550 nm upon excitation at 320 nm (BT2) were monitored for titrations of 0.5 mM CaM in KCl/$CaCl_2$ into 5 μM ligand in 10% MeOH. The conformation of CaM is not significantly affected by the addition of 10% MeOH or 10% DMSO (see below), as determined by measuring ^1H,^{15}H HSQC NMR spectra as a function of solvent composition (data not shown). For ligands BN1 and BN2, titrations of 0.01 mM CaM into 1 μM ligand in 0.1% or 10% DMSO were monitored between 525–575 nm with excitation at 275 nm. Slit widths were 2.5 nm and 5 nm for excitation and emission, respectively. For each ligand, control dilutions of ligand with KCl/$CaCl_2$ solution and of CaM into KCl/$CaCl_2$ solution were performed under the same conditions. The change in fluorescence intensity at 350 nm (MT2), 460 nm (BT2), or 550 nm (BN1, BN2) was used in data fitting to determine the dissociation constants for the interactions.

Determination of Dissociation Contants

Dissociation constants were derived by monitoring chemical shift changes of CaM resonances upon addition of increasing ligand concentrations or ligand fluorescence intensity changes upon addition of increasing CaM concentrations. Data fitting was performed by using n:1 stoichiometry, where n sites are equivalent and independent. Interaction stoichiometries were determined by the model best fitting the data (minimum χ^2 value), both when fitting with integral values for n and when including n as a variable. The fit of the fluorescence data included a slope to accommodate a linear dependence of the fluorescence upon increasing CaM concentration, observed in the control dilutions outlined above.

Isothermal Titration Calorimetry

The enthalpy associated with CaM binding was determined by isothermal titration calorimetry for MT2 and BT1. Experiments were performed on a VP-ITC titration calorimeter (Microcal Inc., Northampton MA). Experiments were performed at least twice. Since BT1 is not soluble at high concentration, dilution of the CaM complex was used to measure the enthalpy of dissociation of the complex. Lyophilized apoCaM was dissolved in unbuffered 100 mM KCl, 4 mM $CaCl_2$, 0.5 mM NaN_3 and dialyzed overnight against the same solution. MT2 or BT1 was dissolved in methanol and added to the stock protein solution (0.4–0.5 mM) to a final concentration of 210 μM for BT1 and 1.4 mM for MT2, and the final methanol content was adjusted to be 5% (v/v). All solutions were degassed for 1 min to minimize evaporation of the methanol. The $(MT2)_2$:CaM or BT1:CaM complex was placed in the syringe. The solution placed in the cell was that used above for the dialysis of CaM, supplemented with 5% methanol, i.e., it is identical to the contents of the syringe, except for the ligand:CaM complex. Aliquots (10–15 μl for MT2 and 15–20 μl for BT1) of the ligand:Cam complexes were added to the cell, and the data were fit to a dissociation isotherm to obtain the stoichiometry (*n*), the enthalpy of binding (ΔH), and the dissociation constant (K_d). The enthalpy associated with dilution of CaM or ligand solutions was also measured by injecting pure ligand and pure CaM solutions separately into the cell, but the effects were small compared with dilution of the complexes. The experiments were repeated at 8°C, 16°C, 25, and 32°C, and the temperature dependence of the enthalpy changes was used to obtain the values of ΔC_p. The high dissociation constant of the monofunctional ligand MT1 resulted in relatively small heat effects, and the data for this ligand are therefore subject to a significantly larger error than are data for the strong binding ligand BT1.

SAXS Measurements

Distance distribution functions were derived as described previously [48]. Protein concentrations exceeded the minimum dissociation constants of the chosen ligand by at least one order of magnitude.

Supplemental Data

Supplemental Data including the characterization of the compounds prepared during this study are available at http://www.chembiol.com/cgi/content/full/12/1/89/DC1/.

Acknowledgments

We thank the Lister Institute, The Wellcome Trust, the Biotechnology and Biological Sciences Research Council, Bender & Co., the Technology Agency of Finland, and the Finnish Academy for financial support; Ritva Serimaa (University of Helsinki) for SAXS measurements; Phillip Nash for some preliminary syntheses; and Accelrys for providing FELIX. J.P.W. is a research fellow of the Lister Institute for Preventive Medicine.

Received: April 26, 2004
Revised: October 30, 2004
Accepted: November 1, 2004
Published: January 21, 2005

References

1. Broom, A.D. (1989). Rational design of enzyme inhibitors: multisubstrate analog inhibitors. J. Med. Chem. *32*, 2–7.
2. Lee, R.T., and Lee, Y.C. (2000). Affinity enhancement by multivalent lectin carbohydrate interaction. Glycoconj. J. *17*, 543–551.
3. Koshland, D.E., Jr. (1962). Comparison of nonenzymic and enzymic reaction velocities. J. Theoret. Biol. *2*, 75–86.
4. Jencks, W.P. (1981). On the attribution and additivity of binding energies. Proc. Natl. Acad. Sci. USA *78*, 4046–4050.
5. Collins, K.D., and Stark, G.R. (1971). Aspartate transcarbamylase. Interaction with the transition state analogue N-(phosphonacetyl)-L-aspartate. J. Biol. Chem. *246*, 6599–6605.
6. Lienhard, G.E., and Secemski, I.I. (1973). P1,P5-Diadenosine-5′pentaphosphate, a potent multisubstrate inhibitor of adenylate kinase. J. Biol. Chem. *248*, 1121–1123.
7. Srinivasan, A., Amarnath, V., Broom, A.D., Zou, F.C., and Cheng, Y.-C. (1984). A potent multisubstrate analog inhibitor of human thymidylate synthetase. J. Med. Chem. *27*, 1710–1717.
8. Kruse, L.I., Kaiser, C., De Wolf, W.E., Jr., Frazee, J.S., Erikson, R.W., Ezekiel, M., Ohlstein, E.H., Ruffalo, R.R., Jr., and Berkowitz, B.A. (1986). Substituted 1-benzylimidazole-2-thiols as potent and orally active inhibitors of dopamine beta-hydroxylase. J. Med. Chem. *29*, 887–889.
9. Yang, I.-Y., Slusher, R.M., Broom, A.D., Ueda, T., and Cheng, Y.-C. (1988). A pyrimidine-based "flexible" bisubstrate analogue inhibitor of human thymidylate synthase. J. Med. Chem. *31*, 2126–2132.

10. Jain, A., Whitesides, G.M., Alexander, R.S., and Christianson, D.W. (1994). Identification of two hydrophobic patches in the active-site cavity of human carbonic anhydrase II by solution-phase and solid-state studies and their use in the development of tight-binding inhibitors. J. Med. Chem. *37*, 2100–2105.
11. Shuker, S.B., Hajduk, P.J., Meadows, R.P., and Fesik, S.W. (1996). Discovering high-affinity ligands for proteins: SAR by NMR. Science *274*, 1531–1534.
12. Huc, I., and Lehn, J.M. (1997). Virtual combinatorial libraries: dynamic generation of molecular and supramolecular diversity by self-assembly.. Proc. Natl. Acad. Sci. USA *94*, 2106–2110.
13. Kramer, R.H., and Karpen, J.W. (1998). Spanning binding sites on allosteric proteins with polymer-linked ligand dimers. Nature *395*, 710–713.
14. Jaenicke, R. (1999). Stability and folding of domain proteins. Prog. Biophys. Mol. Biol. *71*, 155–241.
15. Anderson, H.L., Anderson, S., and Sanders, J.K.M. (1995). Ligand binding by butadiyne-linked porphyrin dimers, trimers and tetramers. J. Chem. Soc. Perkin Trans. I *18*, 2231–2245.
16. Zhang, M., Tanaka, T., and Ikura, M. (1995). Calcium-induced conformational transition revealed by the solution structure of apo calmodulin. Nat. Struct. Biol. *2*, 758–767.
17. Kuboniwa, H., Tjandra, N., Grzesiek, S., Ren, H., Klee, C.B., and Bax, A. (1995). Solution structure of calcium-free calmodulin. Nat. Struct. Biol. *2*, 768–776.
18. Finn, B.E., Evenäs, J., Drakenberg, T., Waltho, J.P., Thulin, E., and Forsén, S. (1995). Calcium-induced structural changes and domain autonomy in calmodulin. Nat. Struct. Biol. *2*, 777–783.
19. Prozialeck, W.C., and Weiss, B. (1982). Inhibition of calmodulin by phenothiazines and related drugs: structure-activity relationships. J. Pharmacol. Exp. Ther. *222*, 509–516.
20. Johnson, J.D., and Wittenauer, L.A. (1983). A fluorescent calmodulin that reports the binding of hydrophobic inhibitory ligands. Biochem. J. *211*, 473–479.
21. Vandonselaar, M., Hickie, R.A., Quail, J.W., and Delbaere, L.T.J. (1994). Trifluoperazine-induced conformational change in Ca2+-calmodulin. Nat. Struct. Biol. *1*, 795–801.
22. Cook, W.J., Leigh, J.W., and Walter, M.R. (1994). Drug binding by calmodulin: crystal structure of a calmodulin-trifluoperazine complex. Biochemistry *33*, 15259–15265.
23. Craven, C.J., Whitehead, B., Jones, S.K.A., Thulin, E., Blackburn, G.M., and Waltho, J.P. (1996). Complexes formed between calmodulin and the antagonists J-8 and TFP insolution. Biochemistry *35*, 10282–10299.
24. Osawa, M., Swindells, M.B., Tanikawa, J., Tanaka, T., Mase, T., Furuya, T., and Ikura, M. (1998). Solution structure of calmodulin-W-7 complex: the basis of diversity in molecular recognition. J. Mol. Biol. *276*, 165–176.
25. Osawa, M., Kuwamoto, S., Izumi, Y., Yap, K.L., Ikura, M., Shibanuma, T., Yokokura, H., Hidaka, H., and Matsushima, N. (1999). Evidence for calmodulin inter-domain compaction in solution induced by W-7binding. FEBS Lett. *442*, 173–177.
26. Persechini, A., and Kretsinger, R.H. (1988). The central helix of calmodulin functions as a flexible tether. J. Biol. Chem. *263*, 12175–12178.
27. Spera, S., Ikura, M., and Bax, A. (1991). Measurement of the exchange rates of rapidly exchanging amide protons: application to the study of calmodulin and its complex with a myosin light chain kinase fragment. J. Biomol. NMR *1*, 155–165.
28. Barbato, G., Ikura, M., Kay, L.E., Pastor, R.W., and Bax, A. (1992). Backbone dynamics of calmodulin studied by 15N relaxation using inverse detected two-dimensional NMR spectroscopy: the central helix is flexible. Biochemistry *31*, 5269–5278.
29. Meador, W.E., Means, A.R., and Quiocho, F.A. (1992). Target enzyme recognition by calmodulin: 2.4 Å structure of acalmodulin-peptide complex. Science *257*, 1251–1255.
30. Meador, W.E., Means, A.R., and Quiocho, F.A. (1993). Modulation of calmodulin plasticity in molecular recognition on the basis of x-ray structures. Science *262*, 1718–1721.
31. Ikura, M., Clore, G.M., Gronenborn, A.M., Zhu, G., Klee, C.B., and Bax, A. (1992). Solution structure of a calmodulin-target peptide complex by multidimensional NMR. Science *256*, 632–638.
32. Braun, S., Kalinowski, H.-O., and Berger, S. (1996). 100 and More Basic NMR Experiments (Weinheim, Germany: VCH).
33. Heidorn, D.B., and Trewhella, J. (1988). Comparison of the crystal and solution structures of calmodulin and troponin C. Biochemistry *27*, 909–915.
34. Heidorn, D.B., Seeger, P.A., Rokop, S.E., Blumenthal, D.K., Means, A.R., Crespi, H., and Trewhella, J. (1989). Changes in the structure of calmodulin induced by a peptide based on the calmodulin-binding domain of myosin light chain kinase. Biochemistry *28*, 6757–6764.
35. Hunter, C.A. (2004). Quantifying Intermolecular Interactions: Guidelines for the Molecular Recognition Toolbox. Angew. Chem. Int. Ed. Engl. *43*, 5310–5324.
36. Calderone, C.T., and Williams, D.H. (2001). An enthalpic component in cooperativity: the relationship between enthalpy, entropy, and noncovalent structure in weak associations. J. Am. Chem. Soc. *123*, 6262–6267.
37. Pozo, D., Reiter, R.J., Calvo, J.R., and Guerrero, J.M. (1997). Inhibition of cerebellar nitric oxide synthase and cyclic GMP production by melatonin via complex formation with calmodulin. J. Cell. Biochem. *65*, 430–442.
38. Benítez-King, G., Huerto-Delgadillo, L., and Antón-Tay, F. (1993). Binding of 3H-melatonin to calmodulin. Life Sci. *53*, 201–207.
39. Vanberkum, M.F.A., and Means, A.R. (1991). Three amino acid substitutions in domain I of calmodulin prevent the activation of chicken smooth muscle myosin light chain kinase. J. Biol. Chem. *266*, 21488–21495.
40. Hui, O.Y., and Vogel, H.J. (1998). Melatonin and serotonin interactions with calmodulin: NMR, spectroscopic and biochemical studies. Biochim. Biophys. Acta *1383*, 37–47.
41. Bayley, P.M., Findlay, W.A., and Martin, S.R. (1996). Target recognition by calmodulin: dissecting the kinetics and affinity of interaction using short peptide sequences. Protein Sci. *5*, 1215–1228.
42. Nyasse, B., Grehn, L., Ragnarasson, U., Maia, H.L.S., Monteiro, L.S., Leito, I., Koppel, I., and Koppel, J. (1995). Synthesis and cathodic cleavage of a set of substituted benzenesulfonamides including the corresponding tert-butyl sulfonylcarbamates: pKa of sulfonamides. J. Chem. Soc. Perkin Trans. I *7*, 2025–2030.
43. Andersson, A., Drakenberg, T., Thulin, E., and Forsen, S. (1983). A 113Cd and 1H NMR study of the interaction of calmodulin with D600, trifluoperazine and some other hydrophobic drugs. Eur. J. Biochem. *134*, 459–465.
44. Vogel, H.J., Lindahl, L., and Thulin, E. (1983). Calcium-dependent hydrophobic interaction chromatography of calmodulin, troponin C and their proteolytic fragments. FEBS Lett. *157*, 241–246.
45. Waltersson, J., Linse, S., Brodin, P., and Grundstrom, T. (1993). Mutational effects on the cooperativity of Ca2+ binding in calmodulin. Biochemistry *32*, 7866–7871.
46. Hajduk, P.J., Olejniczak, E.T., and Fesik, S.W. (1997). One-dimensional relaxation- and diffusion-edited NMR methods for screening compounds that bind to macromolecules. J. Am. Chem. Soc. *119*, 12257–12261.
47. Waltho, J.P., and Cavanagh, J. (1993). Practical aspects of recording multidimensional NMR spectra in water with flat baselines. J. Magn. Reson. Ser. A. *103*, 338–348.
48. Mattinen, M.L., Paakkonen, K., Ilkonen, T., Craven, J., Drakenberg, T., Serimaa, R., Waltho, J., and Annila, A. (2002). Quaternary structure built from subunits combining NMR and small-angle x-ray scattering data. Biophys. J. *83*, 1177–1183.
49. Mohamadi, F., Richards, N.G.J., Guida, W.C., Liscamp, R., Lipton, M., Caufield, C., Chang, G., Hendrickson, T., and Still, W.C. (1990). MacroModel—an integrated software system for modeling organic and bioorganic molecules using molecular mechanics. J. Comput. Chem. *11*, 440–467.
50. Kraulis, P.J. (1991). MOLSCRIPT: a program to produce both detailed and schematic plots of protein structures. J. Appl. Crystallogr. *24*, 946–950.
51. Merritt, E.A., and Murphy, M.E.P. (1994). Raster3D version 2.0. A program for photorealistic molecular graphics. Acta Crystallogr. D Biol. Crystallogr. *50*, 869–873.